Scientia Iranica

Supplementary Information:

Caffeic and Ellagic Acids Simultaneous Spectrofluorometric Analysis by Utilization of Inclusion Complex Formation with γ-Cyclodextrin

Mohammad Abedi*[a], Mohaddeseh Mikani[a], Reza Rahmanian[a]

[a] *Department of Chemical Technologies, Iranian Research Organization for Science and Technology (IROST), P.O. Box 33535-111, Tehran, Iran.*

Corresponding author: E-mail: mabedi50@yahoo.com

Tel: +98 2165276637 fax: +98 2156276265

S1. Temperature and Sonication Time Effects on γ-CD Including EA and CA

The temperature should be one of the important factors dominating thermodynamic and related properties of cyclodextrin inclusion complexes. The present work indicates that the temperature is an important parameter for improving the fluorimetric determination of CA and EA using the inclusion effect of γ-*CD* and further that the efficiency of fluorescence enhancement is affected by the equilibrium and thermodynamic properties of the binding complexes, especially by the entropy changes for complexation. Practically, it can be expected that the fluorescence enhancement efficiency is promoted by using cyclodextrins chemically-modified so as to fit the complex formation of stable but not loose binding with these analytes. Temperature effect on γ-CD including EA and CA is revealed in Fig. S1. It can be realized that in the CA and EA inclusion procedure, the fluorescence intensities reduce slowly as temperature enhances. The extreme fluorescence amounts are at 25 °C based on chemically-modified CA and EA complex formation.

In order to accelerate the inclusion CA and EA on γ-CD, sonication was applied. The sonicating time desired for reaching the inclusion equilibrium depended on the system disturbed. The consequences presented that 10 min reaches the inclusion equilibrium at 65 °C, 15 min at 45 °C, 20 min at 35 °C, and 25 min at 25 °C, correspondingly. Based on these consequences, the 25 °C and 25 min were selected for additional investigation.

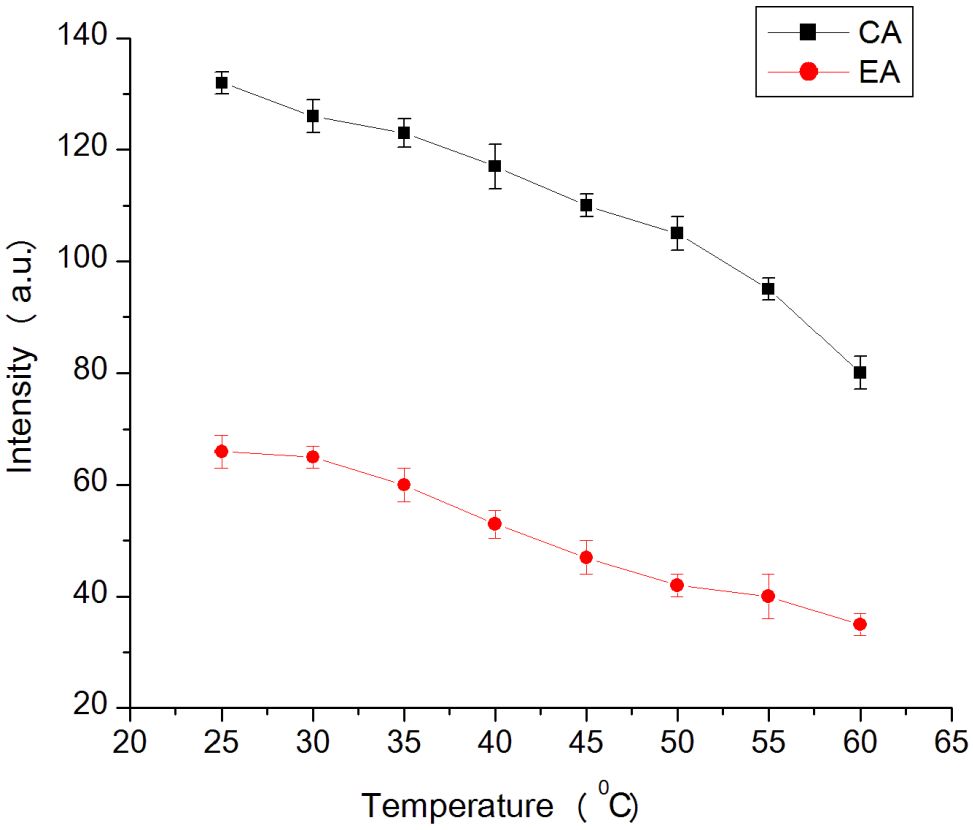

Fig. S1. The fluorescence intensities of CA (1 μg mL^{-1}) and EA (1 μg mL^{-1}) in 0.006 M γ-CD concentration at different temperature values under sonication condition.

S2. CA,EA–γ-CD Complexes Formation Constants

For better investigation in this part we focus on CA–γ-CD. Inclusion formation constant (*K*) was an amount for γ-CD complexing capacity. The formation constants of CA with γ-CD were calculated at various pH values assuming a 1:1 (γ-CD: caffeic acid) inclusion model. The inclusion equilibrium is as surveys:

$$\gamma\text{-}CD + CA \Leftrightarrow CA\text{–}\gamma\text{-}CD \qquad \text{(S1)}$$

The formation constant can be achieved from fluorescence data by the modified Benesi-Hildebrand equation (double the reciprocal plot).

$$\frac{1}{F-F_0} = \frac{1}{(Kk[P]_0[CD]_0)} + \frac{1}{kQ[P]_0} \qquad \text{(S2)}$$

Where F and F_0 represent the fluorescence signals of CA in the γ-CD attendance and absence; $[P]_0$ and $[CD]_0$ display the CA and CD initial concentration; k is an instrumental constant; K is the formation constant of the complex; Q is the quantum yield for the complex. The double reciprocal plots $1/(F-F_0)$ vs. $1/[CD]_0$ for CA to γ-CDs at different value of pH exhibit good linearity (data was not shown). This suggests that the inclusion complexes construction with a stoichiometry of 1:1 (γ-CD: CA). It is noted that the formation constants are very sensitive to the pH values change. One of the main factors disturbing the inclusion interaction is the guest hydrophobicity, which is related to the CA form. CA has four forms: three charged forms and a neutral one. There exists the following equilibrium in aqueous solution (Scheme. S1).

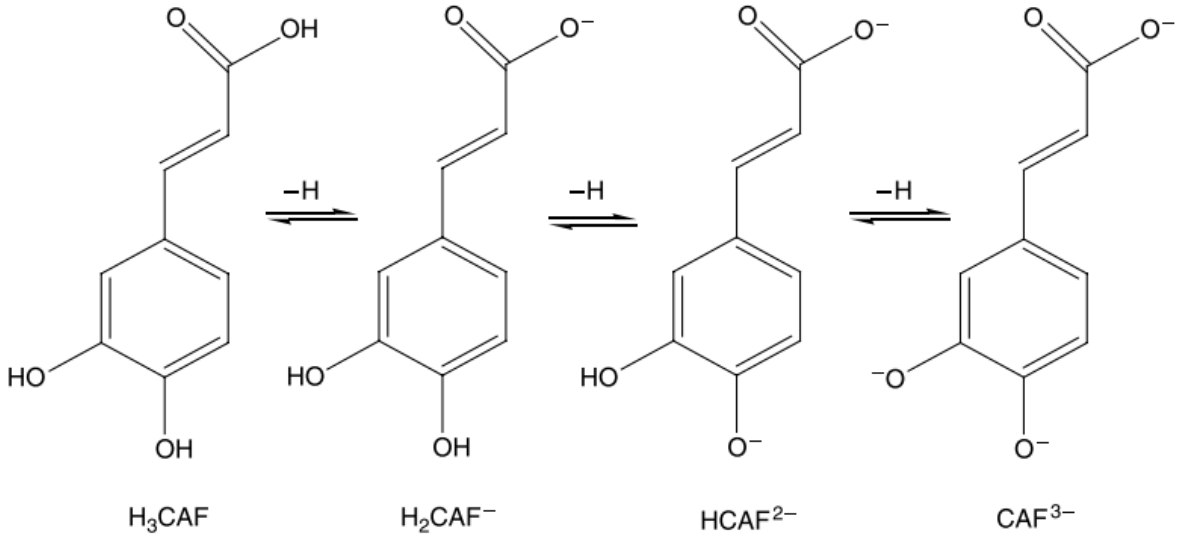

Scheme. S1. The equilibrium of CA in aqueous solution.

The CA neutral form is predominant in pH=2.0-4.5; while pH=5.5-7.4, the charged form of H_2CAF^- is predominant; while pH>8.5, the form of $HCAF^{2-}$ is predominant progressively, and pH>12.5, the CAF^{3-} form is major. As γ-CD cavity is hydrophobic, and the main inclusion interactions are hydrophobic interactions between the γ-CD cavity and guest, the neutral molecules of CA in acidic medium are basically comprised by γ-CD than the related salt of CA in basic medium.

S3. PARAFAC analysis of three way data

10 samples of calibration data and 1 prediction sample were stacked in the direction of sample to obtain a 3-way data set in the PARAFAC analysis. The unknown sample was combined to calibration samples for attaining the second order advantage. Initialization was

achieved by direct trilinear decomposition. The factors number was set as 2 (which are achieved by core consistency) for calibration samples, and 3 are acquired for real samples. In all circumstances, a sensible least squares fit was acquired. The predicted analytes concentration, *RMSEC*, and *RMSEP* in numerous prediction set were considered and informed in Fig. S2, and Table. S1-S3. In this case, BLLS/RBL affords better consequences than PARAFAC. The knowledge behind the BLLS/RBL algorithm can clarify these outcomes, since BLLS/RBL uses concentration info in the calibration stage, a direct least squares procedure to acquire the pure-analyte information and no initialization and constraining processes, yielding analyte profiles and concentrations in samples where robust overlapping happens or little unbilinearity. In conclusion, BLLS/RBL algorithm was selected for data processing to resolve each of the analyte profiles from any uncalibrated interferences which compete with analytes for CD's inclusion complex in subsequent studies.

A

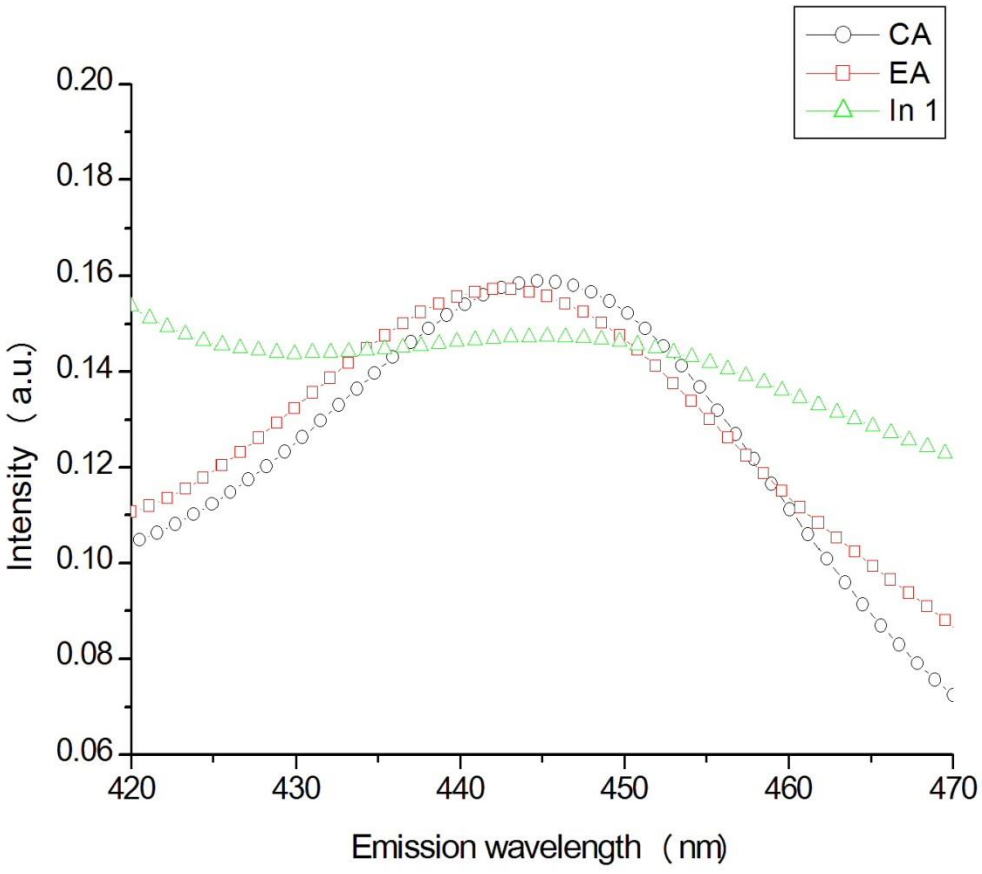

B

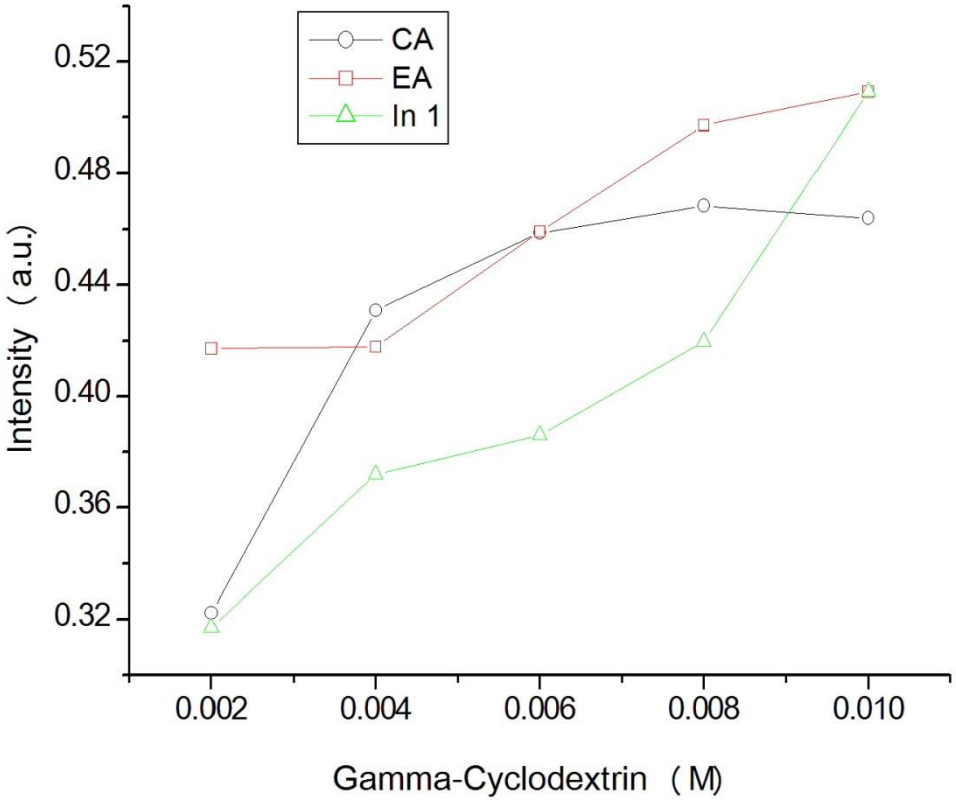

Fig S2. The resolved profiles from PARAFAC for the apple juice.

Table S1

"Calibration samples" for prediction by PARAFAC method.

Samples	CA (μg mL^{-1})		EA (μg mL^{-1})	
	Real concentration	**PARAFAC[a] Result**	**Real concentration**	**PARAFAC Result**
1	3	2	3	2.1
2	4	6.1	2	1.9
3	0	0	6	5.9
4	6	4.9	1	3
5	1	2	7	5.1
6	2	1	4	5
7	0	0	8	9.5
8	5	5.1	0	0
9	7	9.1	0	0
10	2	1.1	5	1.9
RMSEC (μg mL^{-1})	-	1.24	-	1.53

[a] PARAFAC modeling was done using 2 factors as selected by core consistency criterion.

Table S2

"Validation samples" for prediction by PARAFAC method.

Samples NO. (type of interference)	CA (μg mL^{-1})		EA (μg mL^{-1})	
	Real concentration	**PARAFAC[a] Result**	**Real concentration**	**PARAFAC Result**
1 (1 μg mL^{-1} Vanillic acid)	5.5	3.4	0	0
2 (1 μg mL^{-1} Ascorbic acid)	0	0	4.5	4.2
3 (1 μg mL^{-1} Gallic acid)	4.5	6.6	1.5	1
4 (1 μg mL^{-1} Coumaric acid)	1.5	0.6	6	2.9
5 (1 μg mL^{-1} Ferulic acid)	3	2.3	2.5	3.4
6 (1 μg mL^{-1} p-hydroxy benzoic acid)	2.5	2.1	5	6.1
RMSEP (μg mL^{-1})	-	1.43	-	1.54

[a] PARAFAC modeling was carried out using 3 factors as selected by core consistency criterion.

Table S3

"Real samples" for prediction by PARAFAC method and HPLC methods.

Sample no.	Spiked (μg mL^{-1})		PARAFAC[a] Predicted (μg mL^{-1})		HPLC Predicted (μg mL^{-1})	
	CA	EA	CA	EA	CA	EA
Purple Grape juice						
NO. 1	-	-	0.5	2.5	0.9	2
NO. 2	2	-	3.2	1	3	2.01
NO. 3	2	2	3.5	3.1	3	3.98
Strawberries juice						
NO. 1	-	-	4	1.5	3	1.98
NO. 2	1	-	3. 2	1	4.10	1.99
NO. 3	1	2	3.2	4.8	3.99	4.00
NO. 4	2	1	6	2.9	4.99	3.02
Apple juice						
NO. 1	-	-	4.6	2.5	4.99	1.99
NO. 2	1	1	5	4	5.98	2.99
NO. 3	1	-	4.9	1.7	5.97	2.01
NO. 4	-	1	5	2	4.98	2.99

Pomegranate juice						
NO. 1	-	-	1	4.9	1.5	4.50
NO. 2	2	1	2.7	4.5	3.5	5.48
NO. 3	1	1	1.9	5.9	2.49	5.48

[a] PARAFAC modeling was carried out using 3 factors as selected by core consistency criterion.

S4. RSM Analysis

Response surface methodology (*RSM*) includes of a mathematical set and statistical methodologies that are based on the empirical models fit to the investigational data derived in relation to experimental design. The influence of pH, ionic strength, and temperature on CA and EA fluorescence intensity was showed in Table. S4. A response surface model was drawn up and the statistical analysis for the interaction of the three variables (A: pH, B: ionic strength and C: temperature) are offered in Table. S5, Table. S6. The p-value for the model was 0.0001, less than 0.05, which indicated the model was significant and could be employed to display the optimization. The two independent variables, A and C and quadratic terms exerted significant effects CA and EA intensity value within a 95% confidence interval while B doesn't have any effect on the CA and EA intensity based on the model. The parameters of Eq. (S3) and Eq. (S4) given in the experimental section were determined by multiple regression analysis. The following empirical regression equation represents the intensity (a.u.) as a function of pH, and temperature (°C).

$$EA\ intensity\ = +45.25 - 13.90\ \times\ A - 14.91\ \times\ C + 8.75E - 003\ \times\ AC - 9.77 \times\ A^2 - 4.41\ \times\ C^2 \quad \text{(S3)}$$

$$CA\ intensity\ = +107.79 - 33.82\ \times\ A - 25.61\ \times\ C - 1.28\ \times\ AC - 36.66\ \times\ A^2 - 4.68\ \times\ C^2 \quad \text{(S4)}$$

Linear effects of two key variables (*A*, *C*) play a main role in this equation, followed by the quadratic effect of the A^2 and C^2. The intensity could be improved by decreasing linear effect of C and by reducing quadratic effect of B^2.

The optimal conditions of experiment were given by *RSM* as following: pH: 4, temperature: 25°C; Ionic strength: 0.055. Under these conditions, the practical EA and CA intensity were 60 and 125, respectively which was near to the predicted amount intended according to the regression model presented in Eq. (S3, S4). According to the 3D graph (Fig. S3, Fig. S4), the maximal intensity was reached at lower temperature and lower pH.

Table S4

Independent variables and their levels used for central composite design.

Experimental number	pH: (*A*)	Ionic strength (*B*)	Temperature (*C*)	Response	
				CA intensity (a.u.)	EA intensity (a.u.)
1	2	0.1	25	125	32.10
2	2	0.01	25	124.95	45.21
3	2	0.01	60	75.10	60
4	2	0.1	60	75.13	59.95
5	4	0.055	42.5	118.02	36.21
6	6	0.055	42.5	107.07	51.33
7	6	0.055	33.75	116.12	32.10
8	6	0.055	42.5	107.11	45.11
9	6	0.055	42.5	107.10	45.11
10	6	0.055	42.5	107.12	45.19
11	6	0.055	51.25	100.03	37.31
12	6	0.055	42.5	107.09	2.12
13	6	0.0775	42.5	107.12	45.22
14	6	0.0325	42.5	107.13	45.11
15	6	0.055	42.5	107.10	2.24
16	8	0.055	42.5	82.14	45.20
17	10	0.01	25	60.15	29.94
18	10	0.1	25	60.13	49.65
19	10	0.1	60	5.12	45.21
20	10	0.01	60	5.24	30.10

Table S5

Analysis of variance (*ANOVA*) for the fitted quadratic polynomial model for optimization of EA intensity.

Source	Sum of Squares	*df*	Mean Squares	*F* Value	*p*- value Prob> *F*	Result
Model	4431.18	5	886.24	22800.96	< 0.0001	significant
A-pH	1642.29	1	1642.29	42252.44	< 0.0001	
C-Temperature	1891.86	1	1891.86	48673.36	< 0.0001	
AC	6.125E-004	1	6.125E-004	0.016	0.9019	
A^2	23.54	1	23.54	605.68	< 0.0001	
C^2	4.80	1	4.80	123.46	< 0.0001	
Residual	0.54	14	0.039			
Lack of Fit	0.54	9	0.060			
Pure Error	0.000	5	0.000			
Cor Total	4431.73	19				

R-Squared=0.99, Adj *R*-Squared=0.99, Pred *R*-Squared=0.99, [a] *Significant ($p < 0.05$).

Table S6

ANOVA for the fitted quadratic polynomial model for optimization of CA intensity.

Source	Sum of Squares	*df*	Mean Squares	*F* Value	*p*- value Prob> *F*	Result
Model	22980.24	5	4596.05	1001.91	< 0.0001	significant
A-pH	9724.94	1	9724.94	2119.98	< 0.0001	
C-Temperature	5573.38	1	5573.38	1214.96	< 0.0001	
AC	13.06	1	13.06	2.85	0.1137	
A^2	331.33	1	331.33	72.23	< 0.0001	
C^2	5.40	1	5.40	1.18	0.2963	
Residual	64.22	14	4.59			
Lack of Fit	64.22	9	7.14			
Pure Error	0.000	5	0.000			
Cor Total	23044.46	19				

R-Squared=0.99, Adj *R*-Squared=0.99, Pred *R*-Squared=0.99, [a] *Significant ($p < 0.05$).

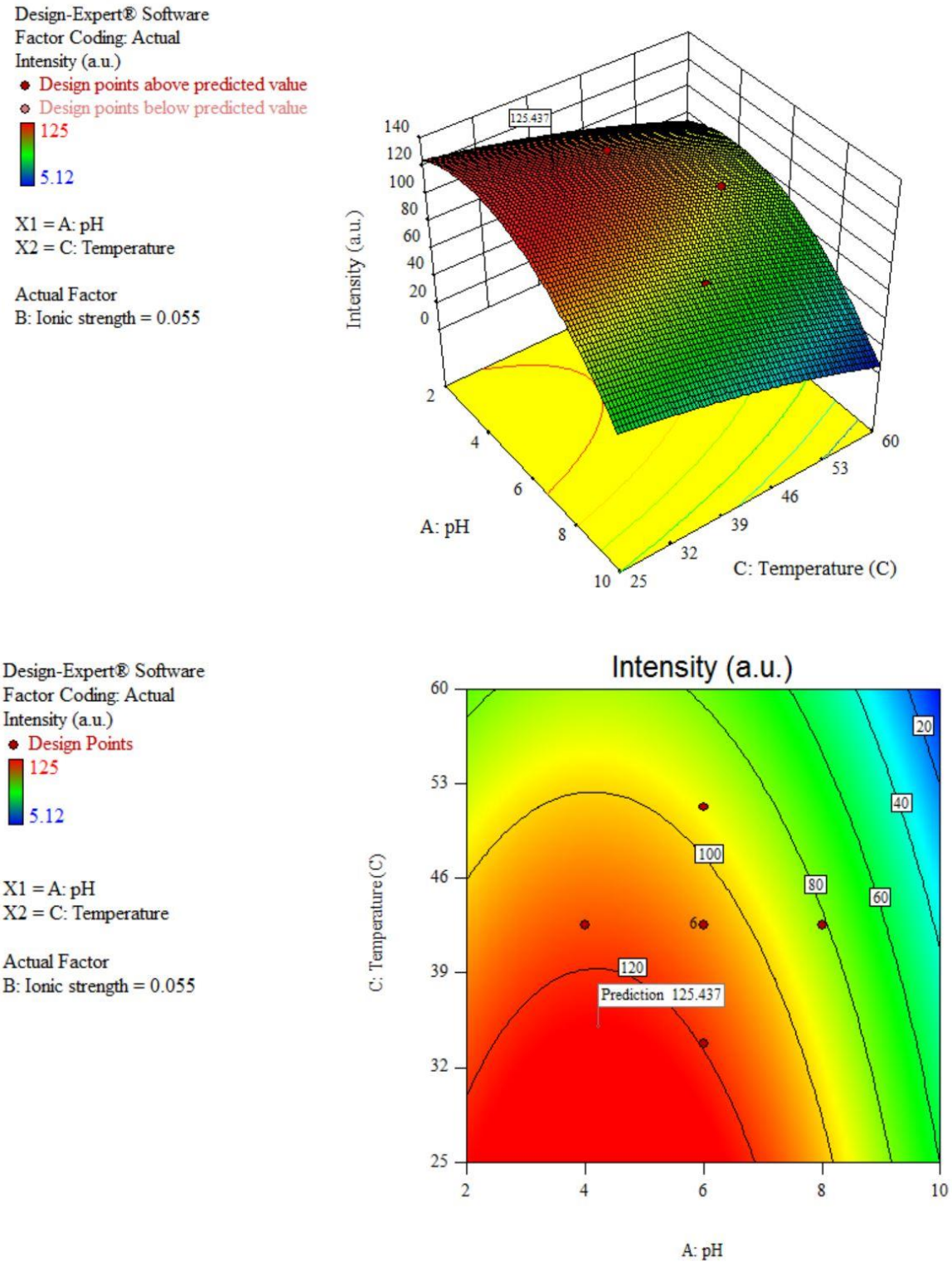

Fig. S3. *RSM* 3D graph for CA.

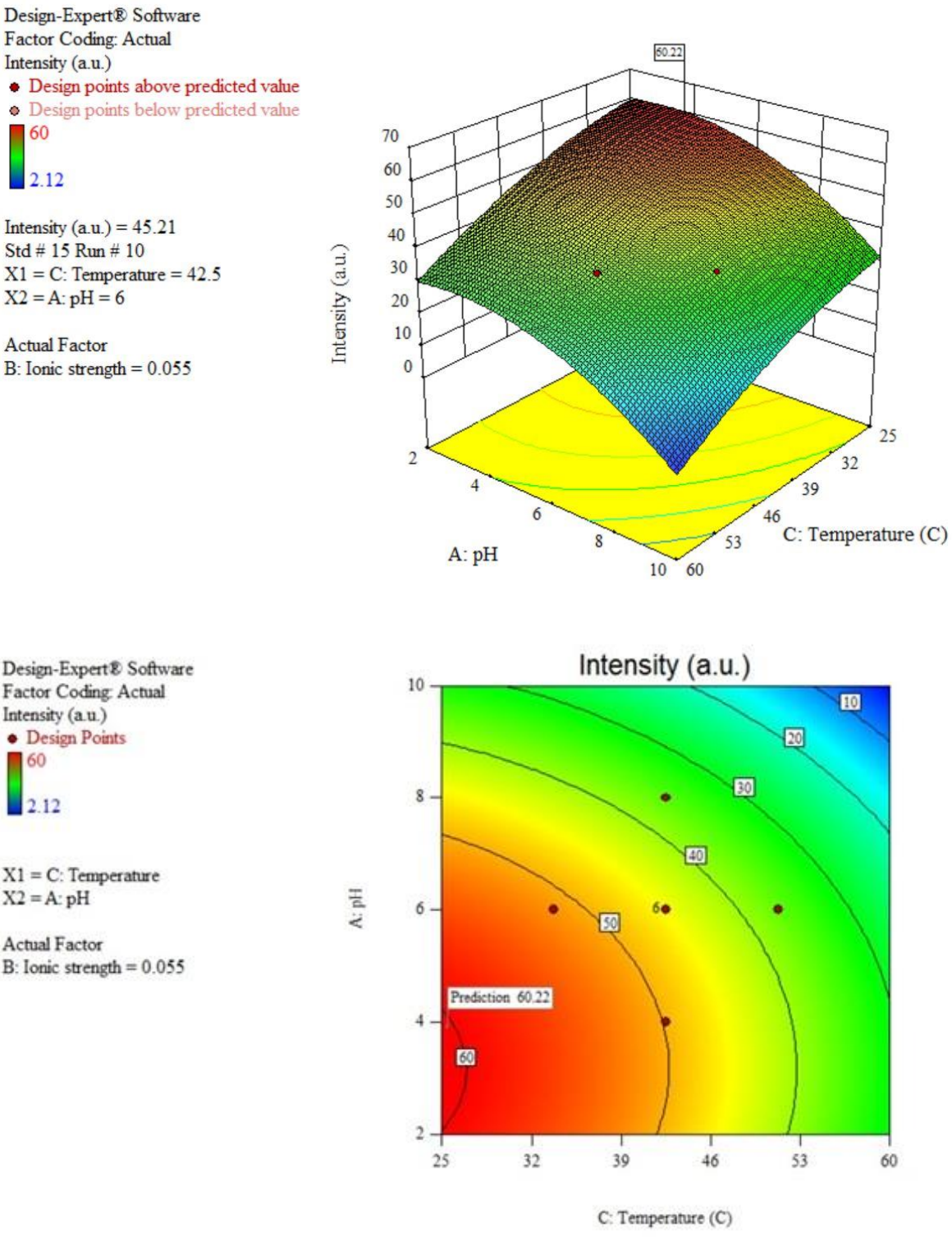

Fig. S4. *RSM* 3D graph for EA.

Abbreviation	Meaning
CA	Caffeic acid
EA	Ellagic acid
γ-CD	γ-cyclodextrin
BLLS/RBL	Bilinear least squares/residual bilinearization
SVD	Singular value decomposition
RBL	Residual bilinearization
LOD	Limit of detection
RMSEC	Root mean squares error of the calibration
RMSEP	Root mean squares error of the prediction
RSM	Response surface methodology
ANOVA	Analysis of variance
PARAFAC	Parallel factor analysis